

show the behaviour shown in Figs 1 and 2 and discussed here. Indeed, motivated by this work, evidence for underlying supernovae in other GRBs is now being reported (GRB970228; ref. 24).

Note added in proof: Galama, T. J. *et al.* (preprint astro-ph/9907264 at <http://xxx.lanl.gov>) (1999) have also recently reported supernova-like behaviour in the light curve and spectrum of GRB970228. □

Received 25 May; accepted 22 July 1999.

1. Kulkarni, S. R. *et al.* The afterglow, redshift and extreme energetics of the γ -ray burst of 23 January 1999. *Nature* **398**, 389–394 (1999).
2. MacFadyen, A. & Woosley, S. E. Collapsars—gamma-ray bursts and explosions in “Failed Supernovae”. Preprint astro-ph/9810274 at <http://xxx.lanl.gov> (1999).
3. Paczynski, B. Are gamma-ray bursts in star-forming regions? *Astrophys. J.* **494**, L45–L48 (1998).
4. Celidonio, G. *et al.* GRB 980326. *IAU Circ.* No. 6851 (1998).
5. Groot, P. J. *et al.* The rapid decay of the optical emission from GRB 980326 and its possible implications. *Astrophys. J.* **502**, L123–L127 (1998).
6. Valdes, F., Jannuzi, B. & Rhoads, J. GRB980326, optical observations. *GCN Circ.* No 56 (1998).
7. Mao, S. & Mo, H. J. The nature of the host galaxies for gamma-ray bursts. *Astron. Astrophys.* **339**, L1–L4 (1998).
8. Hogg, D. W. & Fruchter, A. S. The faint-galaxy hosts of gamma-ray bursts. *Astrophys. J.* **520**, 54–58 (1999).
9. Djorgovski, S. G. *et al.* The optical counterpart of the gamma-ray burst GRB 970508. *Nature* **387**, 876–878 (1997).
10. Sari, R., Piran, T. & Narayan, R. Spectra and light curves of gamma-ray burst afterglows. *Astrophys. J.* **497**, L17–L20 (1998).
11. Mészáros, P., Rees, M. J. & Wijers, R. A. M. J. Viewing angle and environment effects in gamma-ray bursts: sources of afterglow diversity. *Astrophys. J.* **499**, 301–308 (1998).
12. Chevalier, R. A. & Li, Z.-Y. Gamma-ray burst environments and progenitors. *Astrophys. J.* **520**, L29–L32 (1999).
13. Halpern, J. P., Kemp, J., Piran, T. & Bershad, M. A. The rapidly fading optical afterglow of GRB 980519. *Astrophys. J.* **517**, L105–L108 (1999).
14. Sari, R., Piran, T. & Halpern, J. P. Jets in gamma-ray bursts. *Astrophys. J.* **519**, L17–L20 (1999).
15. Piro, L. *et al.* The X-ray afterglow of the gamma-ray burst of 1997 May 8: spectral variability and possible evidence of an iron line. *Astrophys. J.* **514**, L73–L77 (1999).
16. Panaitescu, A., Mészáros, P. & Rees, M. J. Multiwavelength afterglows in gamma-ray bursts: refreshed shock and jet effects. *Astrophys. J.* **503**, 314–324 (1998).
17. Dai, Z. G. & Lu, T. Environment and energy injection effects in GRB afterglows. Preprint astro-ph/9906109 at <http://xxx.lanl.gov> (1999).
18. Li, L. & Paczyński, B. Transient events from neutron star mergers. *Astrophys. J.* **507**, L59–L62 (1998).
19. Galama, T. J. *et al.* An unusual supernova in the error box of the gamma-ray burst of 25 April 1998. *Nature* **395**, 670–672 (1998).
20. Kulkarni, S. R. *et al.* Radio emission from the unusual supernova 1998bw and its association with the γ -ray burst of 25 April 1998. *Nature* **395**, 663–669 (1998).
21. Kirshner, R. P. *et al.* Supernova 1994I in NGC 5194. *IAU Circ.* No. 5981 (1994).
22. Iwamoto, K. *et al.* A hypernova model for the supernova associated with the γ -ray burst of 25 April 1998. *Nature* **395**, 672–674 (1998).
23. Germany, L. M. *et al.* SN 1997cy/GRB 970514—a new piece in the GRB puzzle? Preprint astro-ph/9906096 at <http://xxx.lanl.gov> (1999).
24. Reichart, D. GRB 970228 revisited: evidence for a supernova in the light curve and late spectral energy distribution of the afterglow. *Astrophys. J.* **521**, L111–L115 (1999).
25. Oke, J. B. *et al.* The Keck low-resolution imaging spectrometer. *Publ. Astron. Soc. Pacif.* **107**, 375–385 (1995).
26. Fukugita, M., Shimasaku, K. & Ichikawa, T. Galaxy colors in various photometric band systems. *Publ. Astron. Soc. Pacif.* **107**, 945–958 (1995).
27. Landolt, A. UBVR photometric standard stars in the magnitude range 11.5–16.0 around the celestial equator. *Astron. J.* **104**, 340–371 (1992).
28. Schlegel, D. J., Finkbeiner, D. P. & Davis, M. Maps of dust infrared emission for use in estimation of reddening and cosmic microwave background radiation foregrounds. *Astrophys. J.* **500**, 525–553 (1998).
29. McKenzie, E. H. & Schaefer, B. E. The late time light curve of SN 1998bw associated with GRB980425. *Publ. Astron. Soc. Pacif.* **762**, 964–968 (1999).
30. Schmidt, B. P. *et al.* The high- z supernova search: Measuring cosmic deceleration and global curvature of the universe using type Ia supernovae. *Astrophys. J.* **507**, 46–63 (1998).
31. Massey, P., Strobel, K., Barnes, J. V. & Anderson, E. Spectrophotometric standards. *Astrophys. J.* **328**, 315–333 (1988).
32. Oke, J. B. & Gunn, J. E. Secondary standard stars for absolute spectrophotometry. *Astrophys. J.* **266**, 713–717 (1983).

Acknowledgements

We thank M. H. van Kerkwijk and S. A. Stanford for observations at the Keck II telescope and R. Sari for discussions. We also acknowledge the support from the staff at the Keck Observatory. The observations reported here were obtained at the W. M. Keck Observatory, made possible by the financial support of the W. M. Keck Foundation, which is operated by the California Association for Research in Astronomy, a scientific partnership among California Institute of Technology, the University of California and NASA. S.R.K. and A.V.F. were supported by the NSF and NASA. S.G.D. acknowledges partial support from the Bressler Foundation.

Correspondence and requests for materials should be addressed to J.S.B. (e-mail: jsb@astro.caltech.edu).

.....
Disappearance of stellar debris disks around main-sequence stars after 400 million years

H. J. Habing*, **C. Dominik***, **M. Jourdain de Muizon†**, **M. F. Kessler‡**, **R. J. Laureijs‡**, **K. Leech‡**, **L. Metcalfe‡**, **A. Salama‡**, **R. Siebenmorgen‡** & **N. Trams‡**

* *Leiden Observatory, PO Box 9513, 2300 RA Leiden, The Netherlands*
 † *DESPA, Observatoire de Paris, 92190 Meudon, France and LAEFF-INTA, ESA Vilspa, PO Box 50727, 28080 Madrid, Spain*
 ‡ *Astrophysics Division of ESA, Vilspa, PO Box 50727, 28080, Madrid, Spain*

.....
Almost 5 billion years ago, the Sun formed in a local contraction of a cloud of molecular gas. A rotating disk of gas and dust is believed to have fed material onto the proto-Sun for the first few million years of its life, and to have formed the planets, comets and other Solar System objects. Similar disks, but with less mass, have been observed around a few main-sequence stars such as Vega¹. The dust particles orbiting stars like Vega will be removed on time-scales of the order of 1 Myr (Vega is about 350 Myr old), and therefore must be resupplied¹, at least for a time. But earlier surveys^{2,3} lacked the sensitivity to determine how many nearby stars have dust disks, and to investigate how long such disks survive. Here we report infrared observations indicating that most stars younger than 300 Myr have dust disks, while most older than 400 Myr do not: ninety per cent of the disks disappear when the star is between 300 and 400 Myr old. Several events that are related to the ‘clean up’ of debris in the early history of our Solar System have a similar timescale.

We used the ISOPHOT instrument⁴ on board the ISO satellite⁵, and measured the flux (at wavelengths of 25, 60 and 170 μm) of a sample of 84 nearby main-sequence stars of spectral types A, F, G and K. This sample excludes known multiple, variable or peculiar stars; that is, those for which the interpretation of the infrared emission would be ambiguous. The measurements were reduced using standard software (H.J.H. *et al.*, manuscript in preparation). We checked the quality of our measurements by comparing the measured flux densities with values predicted independently from visual magnitudes (B and V) using an empirical relation derived from IRAS measurements⁶. At 60 μm , the differences between prediction and measurement have a mean value $\mu = 4$ mJy and a dispersion $\sigma = 21$ mJy. The distribution has a pronounced tail

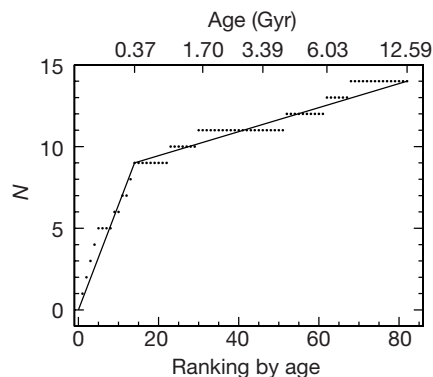


Figure 1 Cumulative distribution of the number of stars that have a disk. All stars are ranked by age. The x-axis shows the rank, and the y-axis the number of stars, N , up to that rank number that have a disk. Some ages are indicated at the top. The two straight lines fit the case when 60% of the stars with rank number lower than 15 (that is, younger than 380 Myr) have a disk and only 9% of the older stars have a disk.

Table 1 Stars younger than 1 Gyr arranged by age

HD	Name	Spectral type	Median age (Myr)	1 σ age limits (Myr)	Disk?
17925		K1V	80	40–150	Yes
30495	58 Eri	G3V	210	160–280	Yes
216956	α PsA	A3V	220	100–340	Yes
102647	β Leo	A3V	240	100–380	Yes
39060	β Pic	A3V	280*	0–520	Yes
20630	κ^1 Cet	G5V	300	180–500	
112185	ϵ UMa	A0p	300	280–1,200	
116842	80 UMa	A5V	320	280–500	
22049	ϵ Eri	K2V	330†	190–540	Yes
37394		K1V	340	270–430	
172167	α Lyr	A0V	350	310–390	Yes
74956	δ Vel	A1V	350	340–380	
95418	β UMa	A1V	360	330–400	Yes
38678	ζ Lep	A2V	370	230–490	Yes
103287	γ UMa	A0V	380	340–400	
15008	δ Hyi	A3V	450	400–500	
106591	δ UMa	A3V	480	420–540	
215789	ϵ Gru	A3V	540	510–580	
156026		K5V	630	440–910	
38392		K2V	650	360–1,100	
12311	α Hyi	F0V	810	780–870	
203280	α Cep	A7IV-V	890	810–980	

HD, identification number in the Henry Draper Catalogue.

* The age of β Pic is controversial; this value is large. See text.

† Age from rotation; calcium emission-line observations suggest²² 800 Myr.

containing stars for which more flux is measured than predicted: these are the stars with Vega-like infrared emission. We conclude that we have detected a disk when the measured flux is larger than the predicted flux by more than $\mu + 3\sigma = 67$ mJy. This gives 14 detections. In the remaining 70 stars, we detected the photosphere or an upper limit close to the photospheric flux. These stars have no disk, or at best a disk significantly fainter than the detected disks. The excellent correlation between predicted and measured flux in most stars confirms that the identification of the infrared source with the star is secure.

We determined an age for each star, and obtained good estimates for 81 of them. (Details of the determinations for 76 stars are reported elsewhere⁷.) For the remaining five stars— ϵ Eridani and four stars from another ISO paper⁸—we determined the age in the same way. The uncertainties in the age determinations are considerable (Table 1). We have taken a rather high value for the age of β Pictoris; a recent determination finds 20 Myr (ref. 9). Had we used that value, our conclusion (see below) would not have changed.

In Table 1 all 22 stars younger than 1 Gyr have been arranged according to increasing median age. The last column contains “yes” when a disk is detected. Below an age of 300 Myr, all stars have a disk. None of the stars in Table 1 older than 400 Myr have a disk, and of the 59 stars older than 1,000 Myr (and not in the table) only 6 have a disk. Future and better determinations of the ages of the stars will undoubtedly lead to a rearrangement of the precise order of the stars in Table 1, but we do not expect that this will change our main conclusion that the typical lifetime of a disk is 300–400 Myr. Figure 1 illustrates this conclusion in a different way (see Fig. 1 legend for details).

Two aspects of our results will be discussed here in more detail: the 300–400 Myr lifetime of the disks, and their disappearance.

We assume that the dust disks do not contain gas, and that the dust particles can move freely. Attempts to measure the gas content of the disk of β Pic¹⁰ justify this assumption. It follows that the dust particles will remain where they are for a time less than 1 Myr, a conclusion reached already in the discovery paper of the disk around Vega¹: radiation pressure will push the smaller particles out of the system, and the Poynting–Robertson effect will bring the larger ones in to where they are vaporized. For β Pic the survival time of the dust at 60 AU is only 4,000 years, and for α Piscis Austrini and Vega (α Lyr) it is 0.1–1 Myr (ref. 11).

If these dust particles are removed within 1 Myr, why do we see

disks with an age of a few hundred Myr? The answer must be: because there is a continuous supply of new dust. Plausible reservoirs of new particles are: collisions between large bodies, and evaporation of comets. Comets will evaporate only when they are within 1 AU or less from the star; the free dust particles will be pushed away to the outer region by radiation pressure. There is direct evidence for the existence of comets near β Pic and in a few other stars: narrow and variable components of the Ca II K-line in absorption suggest the infall of comet-like bodies¹².

We may estimate how much mass is needed for the replenishment. The mass of a disk as seen by ISO is of the order of 0.01 Earth masses^{13,14} ($0.01 M_{\oplus}$). If this disappears in 0.1 Myr and if it is replenished for 400 Myr, then the supply of dust must be $40 M_{\oplus}$ at least. A second, independent, argument leads to an even higher estimate: the collisional equilibrium distribution¹⁵, f , of the particle masses, m , equals $f(m) \propto m^{-1.83}$. If we assume that the largest particles have a size of $a = 100$ km, the total mass is 1.4×10^5 times what we see. If we take $40 M_{\oplus}$ of dust and add gas with a mass 100 times that of the dust, we obtain 0.01 solar masses, a typical value for a disk around a pre-main-sequence star. In other words, by removing its gas and by collecting the dust particles into large planetesimals, a pre-main-sequence disk will have evolved into the type of disk seen by ISO around main-sequence stars.

Are facts known about the history of the disk of our Solar System that correspond to what we know about the dust disks as seen by ISO? Our answer is “yes”. We consider initially the outer Solar System (that is, beyond the orbit of Neptune) because that corresponds to the region where the ISO dust disks are located.

First, model calculations of the formation of Pluto¹⁶, and of the time evolution of the inner Kuiper belt due to collisions¹⁷ and gravitational interaction with Neptune¹⁸, show that current observations are consistent with an early mass of the Kuiper belt of at least 30–50 M_{\oplus} and an initial erosion timescale of 400–800 Myr. Second, it is generally assumed¹⁹ that the Oort cloud of comets formed very shortly after the giant planets. These planets threw ice-covered planetesimals to the outermost regions of the Solar System. Third, the time and the duration of the so-called Late Heavy Bombardment in the inner Solar System coincide with the clean-up phase in the outer Solar System. It is possible, but not yet clear, that these two events are dynamically connected.

We propose that the stars mentioned in Table 1 are in the same phase as was our Solar System when it formed its planets and their satellites, its ring of asteroids, its Kuiper belt and its Oort cloud.

We note that not all debris disks decay after 400 Myr. In about 1 in 11 cases, the disk remains in existence over several Gyr. The disk around the 4.7-Gyr-old G2V star HD207129 is a good example¹⁴. Also, the 4-Gyr-old star ρ^1 Cancri harbours at least one planet²⁰ and a disk^{13,21}. It is currently unclear what causes these disks to live longer than most disks. □

Received 30 March; accepted 30 July 1999.

- Aumann, H. *et al.* Discovery of a shell around Alpha Lyrae. *Astrophys. J.* **278**, L23–L27 (1984).
- Backman, D. E. & Paresce, F. in *Protostars and Planets III* (eds Levy, E. H. & Lunine, J. I.) 1253–1304 (Univ. Arizona Press, Tucson, 1993).
- Gaidos, E. J. Observational constraints on late heavy bombardment episodes around young solar analogs. *Astrophys. J.* **510**, L131–L134 (1999).
- Lemke, D. *et al.* ISOPHOT—capabilities and performance. *Astron. Astrophys.* **315**, L64–L70 (1996).
- Kessler, M. *et al.* The Infrared Space Observatory (ISO) mission. *Astron. Astrophys.* **315**, L27–L31 (1996).
- Plets, H. & Vynckier, C. An analysis of the incidence of the Vega phenomenon among main-sequence and post main-sequence stars. *Astron. Astrophys.* **343**, 496–506 (1999).
- Lachaume, R., Dominik, C., Lanz, T. & Habing, H. J. Age determinations of main-sequence stars: combining different methods. *Astron. Astrophys.* (in the press).
- Ábrahám, P., Leinert, C., Burket, A., Lemke, D. & Henning, T. Search for cool circumstellar matter in the Ursae Majoris group with ISO. *Astron. Astrophys.* **338**, 91–96 (1998).
- Barrado y Navascues, D., Stauffer, J., Song, I. & Caillaut, J. The age of Beta Pic. *Astrophys. J.* (in the press).
- Liseau, R. & Artymowicz, P. On the low gas-to-dust mass ratio of the circumstellar disk around β Pictoris. *Astron. Astrophys.* **334**, 935–942 (1998).
- Artymowicz, P. & Clampin, M. Dust around main-sequence stars: nature or nurture by the interstellar medium. *Astrophys. J.* **490**, 863–878 (1997).

12. Lagrange, A.-M., Backman, D. & Artymowicz, P. Planetary material around main-sequence stars. In *Protostars and Planets IV* (eds Mannings, V., Boss, A. & Russell, S.) (Univ. Arizona Press, Tucson, in the press).

13. Dominik, C., Laureijs, R., Jourdain de Muizon, M. & Habing, H. J. A Vega-like disk associated with the planetary system ρ^1 Cnc. *Astron. Astrophys.* **329**, L53–L56 (1998).

14. Jourdain de Muizon, M., Laureijs, R. J., Dominik, C. & Habing, H. J. A very cold disc of dust around the G0V star HD 207129. *Astron. Astrophys.* (in the press).

15. Dohnanyi, J. Collisional model of asteroids and their debris. *J. Geophys. Res.* **74**, 2531–2554 (1969).

16. Stern, S. A. & Colwell, J. E. Accretion in the Edgeworth-Kuiper belt: forming 100–1000 km radius bodies at 30 AU and beyond. *Astron. J.* **114**, 841–849 (1997).

17. Stern, S. A. & Colwell, J. E. Collisional erosion in the primordial Edgeworth-Kuiper Belt and the generation of the 30–50 AU Kuiper Gap. *Astrophys. J.* **490**, 879–882 (1997).

18. Duncan, M. J., Levison, H. F. & Budd, S. M. The dynamical structure of the Kuiper Belt. *Astron. J.* **110**, 3073–3081 (1995).

19. Weissman, P. in *The New Solar System* 4th edn (eds Beatty, J. K., Petersen, C. C. & Chaikin, A.) 59–68 (Sky Publishing Corp. and Cambridge Univ. Press, Cambridge, Massachusetts, 1999).

20. Butler, R., Marcy, G. W., Williams, E., Hauser, H. & Shirts, P. Three new 51 Pegasi-type planets. *Astrophys. J.* **474**, L115–L118 (1997).

21. Trilling, D. & Brown, R. A circumstellar dust disk around a star with a known planetary companion. *Nature* **395**, 775–777 (1998).

22. Henry, T., Soderblom, D., Donahue, R. & Baliunas, S. A survey of CaII H and K chromospheric emission in southern stars. *Astron. J.* **111**, 439–465 (1996).

Acknowledgements

C.D. was supported by ASTRON, the Stichting Astronomisch Onderzoek Nederland.

Correspondence and requests for materials should be addressed to H.J.H. (e-mail: habing@strw.leidenuniv.nl).

Rapid changes in the mechanism of ocean convection during the last glacial period

Trond M. Dokken*† & Eystein Jansen*‡

* Department of Geology, University of Bergen, Allegt. 41, N-5007 Bergen, Norway

† The University Courses on Svalbard (UNIS), PO Box 156,

N-9170 Longyearbyen, Norway

‡ Nansen Environmental and Remote Sensing Centre, Bergen, Norway

High-amplitude, rapid climate fluctuations are common features of glacial times. The prominent changes in air temperature recorded in the Greenland ice cores^{1,2} are coherent with shifts in the magnitude of the northward heat flux carried by the North Atlantic surface ocean^{3,4}; changes in the ocean's thermohaline circulation are a key component in many explanations of this climate flickering⁵. Here we use stable-isotope and other sedimentological data to reveal specific oceanic reorganizations during these rapid climate-change events. Deep water was generated more or less continuously in the Nordic Seas during the latter part of the last glacial period (60 to 10 thousand years ago), but by two different mechanisms. The deep-water formation occurred by convection in the open ocean during warmer periods (interstadials). But during colder phases (stadials), a freshening of the surface ocean reduced or stopped open-ocean convection, and deep-water formation was instead driven by brine-release during sea-ice freezing. These shifting magnitudes and modes nested within the overall continuity of deep-water formation were probably important for the structuring and rapidity of the prevailing climate changes.

We studied two high-resolution mid-depth sediment cores, IMAGES MD95-2010 and ENAM93-21, from the Nordic Seas. Our main results come from core MD95-2010 (1,226 m depth; 66° 41.05' N, 04° 33.97' E) (Fig. 1), which we compare with results⁶

from core ENAM93-21 (1,020 m depth; 62° 44.3' N, 03° 59.92' W). A striking feature of these records is the high amplitude variability in benthic $\delta^{18}\text{O}$ (Fig. 2; see also Methods), which represents changes occurring at >1 km water depth. Almost identical large $\delta^{18}\text{O}$ variations on millennial timescales are recorded in the two cores. These strong fluctuations in deep water properties occur concomitantly with the rapid climatic changes (D–O cycles) recorded in the Greenland ice cores^{1,2}. Light isotopic events occur during the stadials (cold events), and heavy oxygen isotopic values occur during interstadial (warmer) events. This relationship is documented by the magnetic susceptibility (MS) record which shows detailed correlation with the Greenland ice cores (Fig. 1a, b), and between the cores (Fig. 2a; see Methods). Pronounced maxima (interstadial periods) and minima (stadial periods) in the MS record shift coherently with $\delta^{18}\text{O}$ fluctuations in GISP2. The stadials and interstadials are distinguished by the high content of ice rafted debris (IRD) within the stadials (high content of lithic grains during each stadial event) and by low IRD content during the interstadial events (Fig. 1d, e). Analogues to Heinrich layers, H1 to H6 (refs 3, 4), are identified by a high concentration of lithic grains, and by increased freshening of the surface waters as indicated by light $\delta^{18}\text{O}$

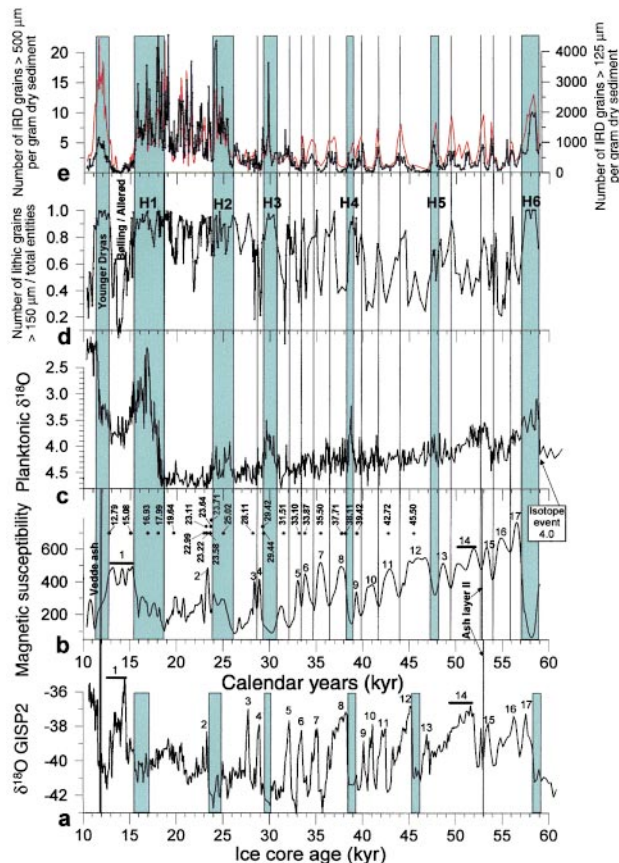


Figure 1 Stratigraphic data sets. Sediment core MD95-2010 versus the GISP2 ice core record. Comparisons of stadal and interstadial events documented from climate proxy data in MD95-2010 (b–e), and from the GISP2 ice core (a) are plotted on individual time scales (see Methods). Corresponding interstadial events (1–17) in the marine record and the ice core are indicated in a and b. a, GISP2 $\delta^{18}\text{O}$ record². b, Magnetic susceptibility (MS) record, with dated levels in MD95-2010 in calendar years indicated. c, $\delta^{18}\text{O}$ record of the planktonic species *N. pachyderma* sin. d, Ratio of lithic grains > 150 μm to the sum of lithic grains and foraminifera. e, Number of lithic grains per gram dry weight sediment. Size fraction > 500 μm shown in black, and size fraction > 150 μm in red. Coloured bars indicate placement of Heinrich-layer analogues, and vertical lines correspond to MS-minima intervals.